# **Environmental** Science Water Research & Technology



**PAPER** 

**View Article Online** 



Cite this: Environ. Sci.: Water Res. Technol., 2019, 5, 1244

Received 14th March 2019, Accepted 17th April 2019

DOI: 10.1039/c9ew00217k

rsc.li/es-water

# Antifouling UV-treated GO/PES hollow fiber membranes in a membrane bioreactor (MBR)†

Mahdi Fathizadeh, 📵 ‡a Weiwei L. Xu, 📵 ‡b Margaret Shen, ‡c Emily Jeng, ‡d Fanglei Zhou, <sup>b</sup> Qiaobei Dong, <sup>D</sup> Dinesh Behera, <sup>b</sup> Zhuonan Song, <sup>a</sup> Lei Wang, <sup>a</sup> Abolfazl Shakouri, <sup>10</sup> a Konstantin Khivantsev<sup>a</sup> and Miao Yu\*b

Single layer graphene oxide (SLGO) was studied as a novel coating material to drastically improve the antifouling performance of polyether sulfone (PES) hollow fiber (HF) membranes in membrane bioreactor (MBR) application. By selectively modifying the membrane surface, only a small amount of SLGO coating (6.2 mg m<sup>-2</sup>) was needed to achieve acceptable membrane performance. The UV treatment of the SLGO coating further assisted in improving the antifouling properties of the as-prepared PES HF membranes. By comparing the transmembrane pressure of pristine PES HF and PES\_GO<sub>6.20</sub>\_UV<sub>X (X = 0-1.5 h)</sub> membranes in a MBR for wastewater treatment at a fixed water flux, the PES\_GO<sub>6.20</sub> UV<sub>1.0</sub> membrane coated with 1 h UV-treated SLGO was demonstrated to substantially relieve the bio-fouling problem. To understand the influence of SLGO modification on membrane performance, FESEM, ATR-FTIR, and AFM analyses were conducted to characterize the as-prepared membranes, and the SLGO deposition mechanism was also proposed in this study.

#### Water impact

Membrane bioreactors (MBRs), which utilize membranes for water filtration from activated sludge, are being widely investigated as an effective method for municipal and industrial wastewater treatment. Current membranes, however, are easily clogged by accumulation of activated sludge on membrane surfaces and/or in pores, and thus suffer from a severe membrane fouling problem, which significantly shortens the lifespan of the membranes and also increases operation cost due to frequent cleaning. There is, therefore, a great need to develop antifouling membranes for highly efficient MBR application. Herein, single layer graphene oxide (SLGO) was studied as a novel coating material to drastically improve the antifouling performance of polyether sulfone (PES) hollow fiber (HF) membranes in membrane bioreactor (MBR) application. By selectively modifying the membrane surface, only a small amount of SLGO coating (6.2 mg m<sup>-2</sup>) was needed to achieve acceptable membrane performance. The UV treatment of the SLGO coating further assisted in improving the antifouling properties of the as-prepared PES HF membranes.

## 1. Introduction

Membrane bioreactors (MBRs), which utilize membranes for water filtration from activated sludge, are being widely investigated as an effective method for municipal and industrial wastewater treatment. Current membranes, however, are easily clogged by accumulation of activated sludge on membrane surfaces and/or in pores, and thus suffer from a severe membrane fouling problem, which significantly shortens the lifespan of the membranes and also increases operation cost due to frequent cleaning. 1-4 There is, therefore, a great need to develop antifouling membranes for highly efficient MBR application.5-7

Among various membranes, polyether sulfone (PES) hollow fiber (HF) membranes have been widely studied in MBR application because of their low cost, excellent stabilities, facile fabrication process, and high surface-to-volume ratio.8-10 The hydrophobic nature of PES, however, makes them more prone to fouling. To improve the hydrophilicity of PES and thus its antifouling performance, hydrophilic nanomaterials, such as TiO2, silica, graphene oxide (GO), and oxidized carbon nanotubes, have been employed as additives. 7,8,11 However, a relatively large amount of additives usually needs to

<sup>&</sup>lt;sup>a</sup> Department of Chemical Engineering, University of South Carolina, Columbia, SC 29208, USA

<sup>&</sup>lt;sup>b</sup> Department of Chemical and Biological Engineering, Rensselaer Polytechnic Institute, Troy, NY 12180, USA. E-mail: yum5@rpi.edu

<sup>&</sup>lt;sup>c</sup> Science, Mathematics, and Computer Science Magnet Program, Montgomery Blair High School, 51 University Blvd E, Silver Spring, MD 20901, USA

<sup>&</sup>lt;sup>d</sup> School of Chemical and Biomolecular Engineering, Cornell University, Ithaca,

<sup>†</sup> Electronic supplementary information (ESI) available: AFM image of SLGO flakes; ATR-FTIR of SLGO, UV-treated SLGO, pristine PES HF and SLGO/UVtreated SLGO coated PES HF membranes: the pore size distribution of PES HF membranes; FESEM and AFM topological scans of PES HF membranes. See DOI: 10.1039/c9ew00217k

<sup>‡</sup> These authors contributed equally.

be uniformly dispersed in the whole polymer membranes to obtain improved surface hydrophilicity. This not only increases the material cost, especially for expensive additives, but also potentially changes the mechanical stability of membranes. In contrast, surface modification has been shown as an effective way to selectively modify membrane surface hydrophilicity. Compared with various methods, 12-17 depositing ultrathin hydrophilic coatings by facile solution phase deposition methods may effectively enhance membrane surface hydrophilicity while maintaining the bulk polymer characteristics. 18,19

In recent years, GO has attracted lots of attention as a promising two-dimensional coating material, owing to its one carbon atom thickness, ease of conformation to substrates, excellent chemical stability, and mechanical strength.20-26,34 Besides, it has also been tested as an effective additive to improve the antifouling performance of PES membranes. For example, Lee et al.27 and Jin et al.28 prepared mixed matrix membranes by uniformly mixing GO with PES for wastewater treatment and for oil/water separation. Their results indicated that GO significantly increased the hydrophilicity of PES membranes and substantially improved water flux.<sup>27</sup> However, a large amount of GO, around 2.5 wt% relative to the polymer weight, was needed to achieve significant improvement, with most of the GO flakes being embedded inside the PES membranes. Therefore, it would be highly desirable to selectively deposit GO flakes only on the PES membrane surface to drastically lower the amount of GO required to improve surface hydrophilicity. In addition, we found that UV treatment increased the O/C ratio in GO flakes and thus effectively improved hydrophilicity of GO coatings. Applying UV-treated GO coatings on PES may further improve the surface hydrophilicity. 7,28,29 Thus, herein, we first investigated the effect of surface modification with GO coatings on improving the antifouling performance of PES HF membranes in membrane bioreactor application. The antibiofouling ability of GO deposited PES HF membranes was evaluated with both simulated foulants and activated sludge provided by the local industry. Besides, since UV treatment for GO flakes is a facile way to increase the GO hydrophilicity, we also applied UV treated GO coatings to improve the antifouling performance of PES HF membranes.

#### 2. Materials and methods

## 2.1 Single layer GO (SLGO) dispersion preparation and coating deposition

The PES HF (diameter: 6 mm) with a molecular weight cutoff (MWCO) of around 150 kDa was purchased from Hydranautics-Nitto Group Company. The selective PES layer is on the external surface of the HF. SLGO was purchased from Cheap Tubes, Inc. (Brattleboro, VT, USA), and SLGO dispersion was prepared by the following procedure. One gram of SLGO was added in 1 liter of deionized water and subsequently sonicated for 2 h. After sonication, the SLGO dispersion was centrifuged at 8000 rpm for 1 h to remove large

aggregates and obtain the SLGO dispersion. The UV-vis spectrum of the SLGO dispersion was then measured, and the SLGO concentration in the as-prepared dispersion was determined by a calibration curve using standard GO dispersions. The obtained SLGO stock dispersion was appropriately diluted to obtain the SLGO coating dispersion with a concentration of  $1.91 \times 10^{-4}$  mg mL<sup>-1</sup>. An UV lamp (B-100Y, Mineralogical Research Company) was used to treat the SLGO flakes to produce more hydrophilic SLGO. Specifically, the SLGO dispersion was vigorously stirred under UV irradiation with different times.

A facile vacuum filtration method was used to deposit SLGO and UV-treated SLGO on PES HFs. Before filtration, one end of the PES HFs was sealed with epoxy, and the other end was connected to a vacuum pump. These HFs were then put into the SLGO and UV-treated SLGO dispersions for the filtration coating. The pressure drop across the membrane was fixed to 30 kPa. SLGO loading amounts (mg m<sup>-2</sup>) and UV treatment times for different membranes are listed in Table 1. SLGO coated PES HF membranes were dried under vacuum for 12 h at 60 °C before being used for filtration tests.

#### 2.2 Membrane characterization

The surface functional groups of the SLGO (with and without UV treatment) coated PES HF membranes and uncoated PES HFs were characterized by attenuated total reflection-Fourier transform infrared spectroscopy (ATR-FTIR) analysis. ATR-FTIR spectra were collected on a Nicolet 6700 FTIR spectrometer (Thermo Scientific, Waltham, MA, USA) over the range of 800-4000 cm<sup>-1</sup>. The dried PES HF membranes were placed on a glass substrate, and then the laser beam was focused on the center of the membrane surface.

The surface morphologies and pore sizes of the PES HF membranes were examined with a field emission scanning electron microscope (FESEM) (Zeiss UltraPlus, Germany). The pore size distribution was calculated using ImageJ. Samples as shown in the cross-sectional SEM images were prepared by immersing the PES HF membranes in liquid nitrogen for several minutes, and then were broken into small rings with sharp edges. The surface roughness of the pristine PES HFs and SLGO coated PES HF membranes was measured by

Table 1 Preparation and post-treatment conditions for SLGO coated PES HF membranes

Membrane	GO content (mg m <sup>-2</sup> )	UV treatment time (h)
PES	0	0
$PES\_GO_{1.55}$	1.55	0
PES_GO <sub>3.10</sub>	3.10	0
$PES\_GO_{6.20}$	6.20	0
PES_GO <sub>9.31</sub>	9.31	0
$PES\_GO_{6.20}\_UV_{0.5}$	6.20	0.5
$PES\_GO_{6.20}\_UV_{1.0}$	6.20	1.0
$PES\_GO_{6.20}\_UV_{1.5}$	6.20	1.5

atomic force microscopy (AFM) (AFM Workshop, CA, USA), and average results from five measurements were reported.

#### 2.3 Membrane filtration measurements

Membrane filtration performance was investigated by using the PES HFs with a total filtration area of  $\sim 10 \text{ cm}^2$  in the MBR system (Fig. 1). During filtration measurements, The PES HF membranes were directly submerged in the MBR, and the total flux through the HFs with and without the presence of foulants in the feed solution was determined under a constant pressure drop of around 30 kPa controlled using a vacuum pump and an adjustable venting needle valve. Continuous air flow was introduced using an air blower placed at the bottom of the liquid tank through an air diffuser. Air flow can remove solid accumulation on the PES HF surface and supply the required oxygen for the microorganisms. The SLGO coated PES HF membranes and uncoated HFs were tested for at least 4 h to obtain steady state results. Bovine serum albumin (BSA >98%, purchased from Sigma Aldrich), sodium alginate (SA), and silicon dioxide (SiO2) particles were selected as model foulants to investigate the antifouling performance of the pristine PES HFs and SLGO coated PES HF membranes. Table 2 summarizes the particle size of these foulants and concentration of the foulants in the feed solution (top). Single-foulant filtration measurements were used to investigate the effect of SLGO loading and UV treatment time on the antifouling properties of the PES HF membranes.

The optimized SLGO coated PES HF membrane was used for membrane MBR testing; during the test, a constant flux operation mode was adopted, while the transmembrane pressure was monitored (Fig. 1). Constant permeation flux was controlled by adjusting the pressure of the vacuum pump using a needle valve. The simulated wastewater was prepared by mixing 5 g L<sup>-1</sup> of skim milk, 5 g L<sup>-1</sup> of sucrose, 0.1 g L<sup>-1</sup> of MgSO<sub>4</sub>, and 0.1 g L<sup>-1</sup> of NH<sub>4</sub>Cl.<sup>30</sup> The activated sludge was provided by the City's Metropolitan Wastewater Treatment Plant (Columbia, SC, USA) with a mixed liquor suspended solid (MLSS) concentration of 8000 mg L<sup>-1</sup>. In the designed MBR, the volume, aeration rate, permeation flux and food-tomicroorganism (F/M) ratio were fixed at 1 L, 1 L min<sup>-1</sup>, 20 L

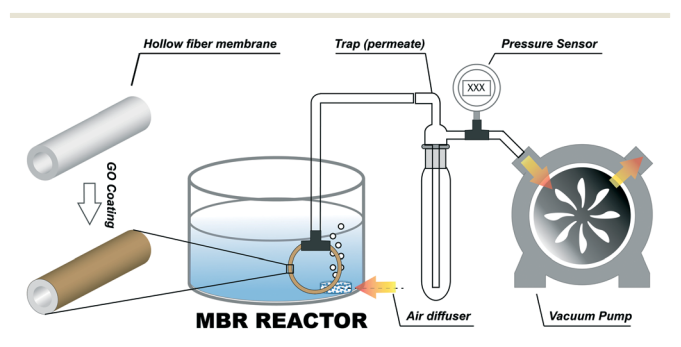


Fig. 1 Schematic illustration of the lab scale membrane bio-reactor (MBR).

Table 2 The component of wastewater for the fouling test and the condition for long term MBR testing

	Concentration	Particle size
Foulants	$(\text{mg L}^{-1})$	(nm)
Bovine serum albumin	50	550
Sodium alginate	50	240
Silicon dioxide particle	1000	1500
MBR testing condition		
Reactor volume	1	Liter
MLSS	8000	${ m mg~L}^{^{-1}}$
Feed concentration (TOC)	2000	ppm
F/M ratio	0.2	_
pH	~7	
Membrane area	10	cm <sup>2</sup>
Sludge source	Metropolitan Wastewater	
_	Treatme	ent Plant,
	Columb	oia, SC, USA

(m<sup>2</sup> h)<sup>-1</sup> and 0.2, respectively. The operation condition of the MBR is given in Table 2 (bottom). A total organic carbon (TOC) analyzer was used to measure the concentration of carbon in both feed and permeate sides. TOC concentration was measured by two analyses: one to measure total carbon (TC), and the other to measure inorganic carbon (IC). The difference between these two measurements is the TOC concentration. For this approach, 20 mL of MBR permeate was used for TOC analysis (Tekmar Phoenix 8000-Persulfate TOC analyzer). Reported TOC for every 4 h was tested three times.

## Results and discussion

#### 3.1 SLGO coatings on the PES membrane surface

In this work, the SLGO dispersion was prepared through long term sonication, followed by high speed centrifugation. The single layer feature of the as-prepared GO flakes was confirmed by the AFM image shown in Fig. S1a,† and the lateral size of the SLGO flakes was around 0.7-1.3 μm. Fig. S1b† exhibits the ATR-FTIR spectrum of SLGO dispersed in water; the characteristic peaks of -C=O, -C-OH (carboxyl functional groups) and C=C stretching were detected at 1720, 1430, and 1540-1620 cm<sup>-1</sup>, corresponding well to the typically reported GO structure and indicating the presence of pristine graphic carbon and various hydrophilic functional groups on the SLGO flakes.

To fabricate SLGO deposited PES HF membranes, a facile vacuum filtration method was applied, and the detailed process was described in the Materials and methods part. Since the PES HF has small pores (~300 nm), medium pores (~860 nm) and large (~1300 nm) pores that split into smaller pores below the surface (see discussion for Fig. 3 below), three sequential stages might exist during the overall SLGO deposition process, as proposed schematically in Fig. 2. In the first stage, SLGO is expected to deposit on the surface of the small pores, diffuse to the inside of the large pores, and partially cover the edge of the medium pores. In the second stage,

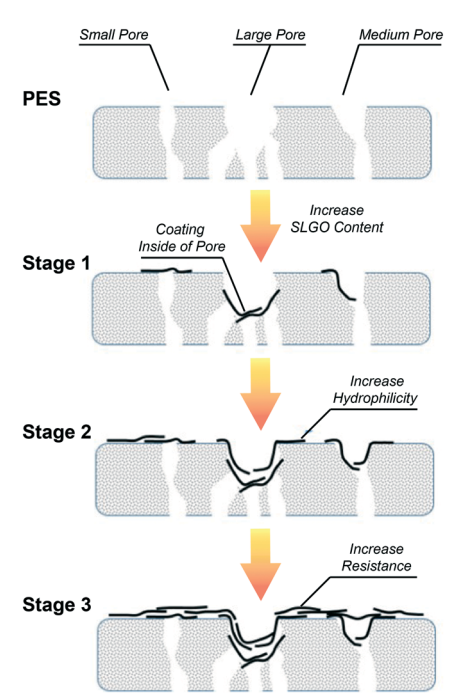


Fig. 2 Proposed SLGO coating mechanism on the PES hollow fiber membrane

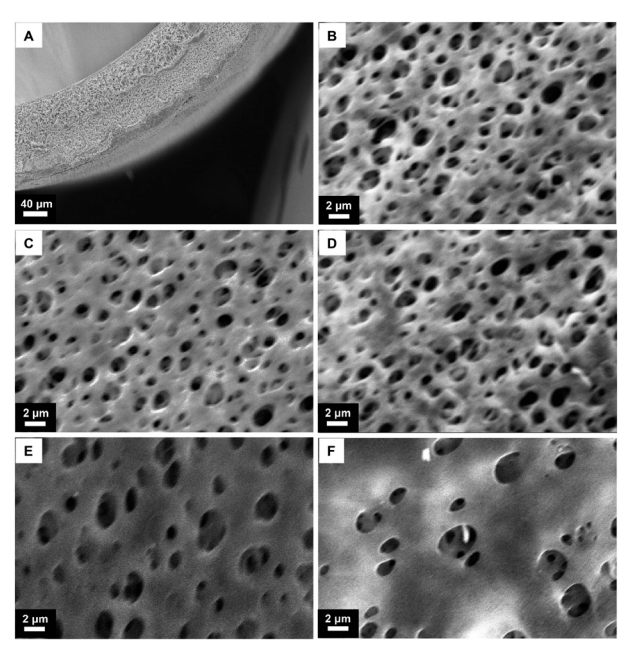


Fig. 3 The FESEM images of pristine PES HF and SLGO coated PES HF membranes: (A) cross sectional SEM image of the pristine PES HF; (B) surface SEM image of the pristine PES HF; and surface SEM images of the PES HF coated with (C) 1.55, (D) 3.10, (E) 6.20, and (F) 9.31 mg m<sup>-1</sup> of SLGO flakes.

with the increasing loading of SLGO, most of the membrane surface would be covered with the SLGO flakes, which could increase the hydrophilicity of the PES membrane. In this stage, the loading of SLGO should be optimized to generate the lowest mass transfer resistance while greatly improving the hydrophilicity of the membrane surface. In the third stage, as the SLGO flakes keep stacking on the PES membrane surface, the permeance of the membrane would decrease because of the increased transport resistance. In this work, we fabricated PES HF membranes with different loadings of SLGO and UV-treated SLGO (Table 1) and studied their influence on the membrane separation performance and antifouling ability in the MBR.

ATR-FTIR was first applied to characterize the pristine PES HF and SLGO coated PES HF membranes. As shown in Fig. S2,† the pristine PES HF showed characteristic peaks at 1578 and 1485 cm<sup>-1</sup>, which can be assigned to the aromatic C=C bond and C-C bond stretching. The phenyl ether bond of PES appeared at around 1240 cm<sup>-1</sup> and was observed in all the membranes. Besides that, absorption peaks at 1320 and 1150 cm<sup>-1</sup> were attributed to asymmetric and symmetric stretches of the sulfone group (SO2) in PES, which is consistent with the characterization results of the PES membranes reported in the literature. 15 After SLGO coating, new peaks at 1220, 1540, 1720, and 2950 cm<sup>-1</sup>, corresponding to the epoxy, carboxyl, and aromatic functional groups of SLGO, were clearly observed. The relative intensity of the carboxyl or epoxy groups to the SO<sub>2</sub> group can reflect the increase of SLGO loading on the PES surface; with the increase of SLGO loading on the PES HF from 1.55 to 9.31 mg m<sup>-2</sup>, the ratio of the carboxylic acid group to the SO<sub>2</sub> group gradually increased.

FESEM was carried out to investigate the surface morphology of the pristine PES HF and SLGO deposited HF membranes (Fig. 3). Fig. 3A and B illustrate that the PES HF had a continuous porous structure, and the HF surface had pores with a size in the range from 0.2 to 1.7 µm. With the increase of SLGO loading on the PES HF (Fig. 3C-F), a number of pores decreased and most of the smaller pores were covered with the SLGO flakes. To further investigate the SLGO coating process, FESEM was performed using ImageJ to obtain the trend of pore size distribution change with SLGO loading. As shown in Fig. S3,† the pristine PES HF showed three pore size peaks located at 300, 860 and 1300 nm. With the increase of SLGO loading, the small pores (300 nm) started to disappear; as SLGO loading increased to 3.1 mg m<sup>-2</sup>, the small pores were totally covered, and the relative amount of medium pores (860 nm) started to drop; when the SLGO loading further increased to 6.2 and 9.31 mg m<sup>-2</sup>, the medium sized pores were mostly covered, and the amount of uncovered large pores (1300 nm) was reduced significantly. As a result, the extra-large pores (>1500 nm) which account for very small portions on the pristine PES HF gradually played the dominant role, and the corresponding pore size distribution peak shifted to a larger size as well.

The pore size distribution change with SLGO loading can further support the proposed deposition mechanism on PES HFs. Since the SLGO flakes had a lateral size ranging from 0.7 to 1.3  $\mu$ m, at small SLGO loading (1.55 mg m<sup>-2</sup>), most of the SLGO flakes entered the large pores, and only the pores smaller than the size of the SLGO flakes could be covered (Fig. S3†). Accordingly, the surface hydrophilicity of the SLGO

coated HF was not expected to improve significantly due to the insufficient coverage of the membrane surface. With the increase of SLGO loading (>3.1 mg m $^{-2}$ ), most of the small and medium pores were covered, and the edge of the large pores started to be coated by the SLGO flakes as well. At this stage of coating, the SLGO deposited PES HF is expected to have a uniform coating layer, which could balance the surface hydrophilicity and transport resistance and thus reduce membrane fouling while keeping the permeance high. However, after passing this optimal point, the increase of the GO loading (9.10 mg m $^{-2}$ ) increased the coating layer thickness and covered more large pores, leading to the decreased permeance of the membrane.

In addition to membrane surface hydrophilicity, surface roughness is another important property related to membrane fouling; usually, a rougher membrane surface is more susceptible to fouling and more difficult to clean. To study the surface roughness change with SLGO loading, AFM was conducted to scan the surface of the PES HF before and after SLGO coating. Fig. 4 shows that as the SLGO loading increased from 1.55 to 6.20 mg m<sup>-2</sup>, the surface of the PES HF became smoother, and the surface roughness gradually reduced from 44 to 33 nm (Table 3), which is in good agreement with the FESEM and pore size distribution results that

Table 3 Surface roughness of pristine HF and SLGO coated PES HF membranes

Membrane	Ra (nm)	Rms (nm)
PES	44.2	54.0
PES_GO <sub>1.55</sub>	40.9	51.4
PES_GO <sub>3,10</sub>	39.2	48.0
PES_GO <sub>6,20</sub>	33.1	38.1
PES_GO <sub>9.31</sub>	38.2	47.5
PES_GO <sub>6.20</sub> _UV <sub>0.5</sub>	34.2	39.4
PES_GO <sub>6.20</sub> UV <sub>1.0</sub>	38.4	42.6
PES_GO <sub>6,20</sub> _UV <sub>1.5</sub>	37.8	41.7

most of the surface pores (small and medium size) were covered by the SLGO flakes. However, when 9.31 mg m $^{-2}$  SLGO was deposited on the PES HF, the increased surface roughness was simply due to the overloading of SLGO on the membrane surface. Fig. 4F exhibits the AFM image of a selected area where one SLGO flake was clearly scanned, indicating that the SLGO flakes can completely conceal the small/medium pores and partially cover the big pores. Fig. S4† also shows the 2D AFM images of the UV-treated membranes. A comparison between PES\_GO $_{\rm 6.20}$  and that with UV-treatment shows that surface roughness increased after UV-treatment. UV-treatment can create big holes on the GO flakes, which

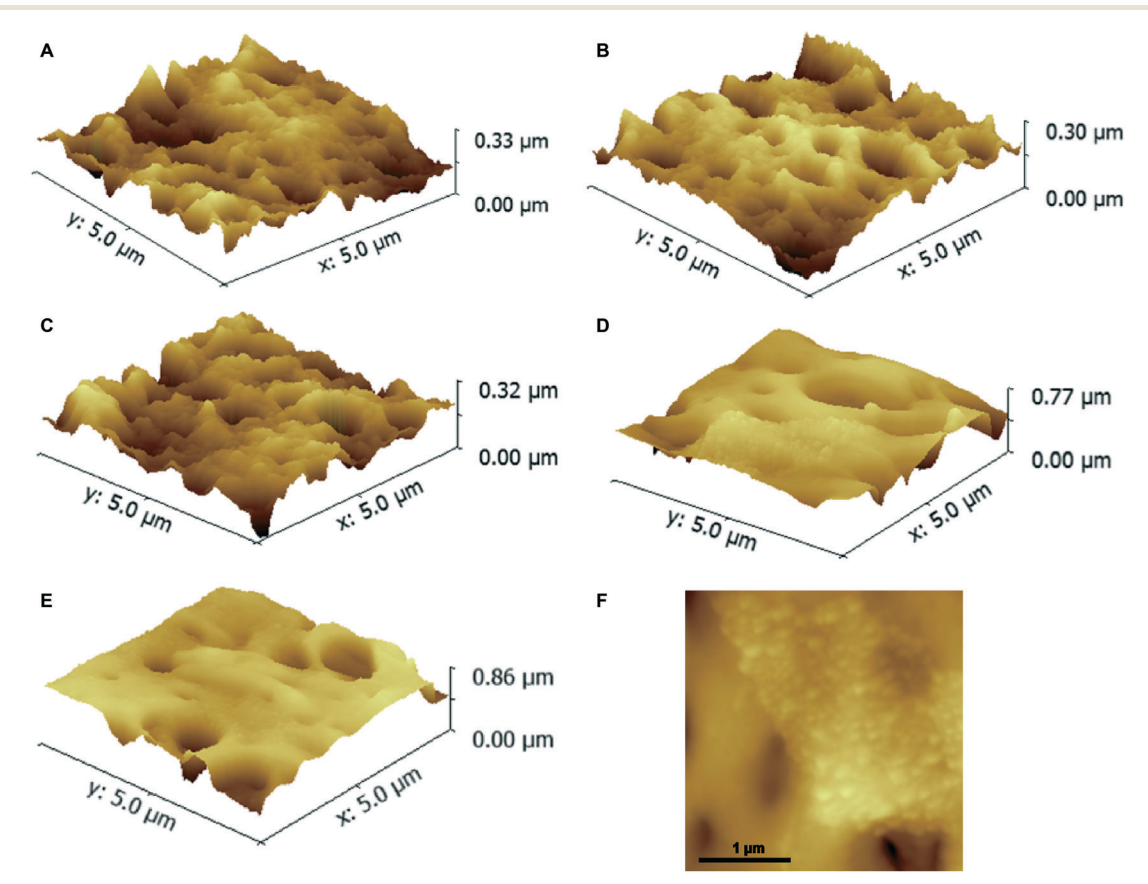


Fig. 4 AFM topological scan of pristine PES HF and SLGO coated PES HF membranes: (A) 3D AFM image of the pristine PES HF; (B)–(E) 3D AFM images of the PES HF coated with 1.55, 3.10, 6.20, and 9.31 mg m $^{-2}$  of SLGO flakes, respectively; (F) AFM image of the GO flake covered on the PES HF surface and pores (PES $_{-6.20}$  membrane).

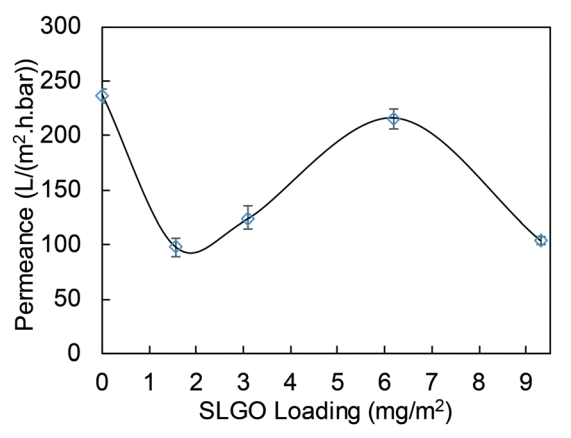


Fig. 5 Pure water permeance of pristine PES HF and PES HF membranes deposited with different SLGO loadings.

causes the increase of the surface roughness. After 1.5 UVtreatment, the surface roughness slightly decreased from 43 to 41 nm, probably resulting from the smaller GO flakes after UV irradiation. 19

#### 3.2 Effect of SLGO coating on pure water permeation and antifouling performance

High permeance and good antifouling performance are two desired properties for membranes used in MBR applications. Therefore, the effect of SLGO loading on pure water permeation and antifouling performance of the PES HF membranes was investigated. The pure water permeance of the uncoated PES HF and SLGO deposited PES HF membranes is shown in Fig. 5. With the increase of SLGO loading, water permeance decreased initially and then increased with SLGO loading; as more than 6.20 mg m<sup>-2</sup> of SLGO was deposited on the PES HFs, the water permeance of the membrane decreased again. The combined effect of the two factors, surface hydrophilicity and transport resistance, could be used to explain the water permeation performance of the SLGO coated PES HF membranes. 5,27,32,33 When SLGO loading was low, such as 1.55 mg m<sup>-2</sup>, surface hydrophilicity was not improved significantly enough to balance the transport resistance generated by the

covering of small PES HF pores (mechanism explained in 3.1), therefore leading to a decrease of water permeance from 243 to 98 L (m<sup>2</sup> h bar)<sup>-1</sup>. By further increasing the SLGO loading to 3.10 and 6.20 mg m<sup>-2</sup>, the improved surface hydrophilicity gradually dominated the water transport in the PES HF membranes, and the water permeance started to increase. However, as the SLGO loading increased to 9.31 mg m<sup>-2</sup>, the surface hydrophilicity could not make up for the greatly increased transport resistance, and thus the water permeance decreased. Therefore, 6.20 mg m<sup>-2</sup> of SLGO coating seems to be the optimum point where the surface hydrophilicity and transport resistance could be effectively balanced.

During the membrane separation process, membrane fouling is unavoidable, and foulant particles could stick on the membrane surface, block pores and lead to the loss of permeance. However, a layer of GO coating could mitigate the adhesion of foulants to the membrane surface and thus improve the membrane antifouling ability. Therefore, the antifouling performance of the SLGO coated PES HF membranes was firstly investigated using three model foulants: SiO<sub>2</sub> particles, BSA, and sodium alginate (Fig. 6). When using SiO<sub>2</sub> particles as the model foulant, the permeance of the pristine PES HF decreased to ~55% during the filtration test, while the maximum permeance drop for the SLGO coated HF membranes was only around 25%. A similar trend was observed in filtration tests using BSA and sodium alginate as foulants. As shown in Fig. 6, by testing all three model foulants, the PES\_GO<sub>6.20</sub> membrane coated with 6.20 mg m<sup>-2</sup> of SLGO exhibited the highest permeance over the whole filtration period, apparently resulting from its well-balanced surface hydrophilicity and transport resistance (as discussed above). After 4 h of the fouling test, the permeance measured for the PES\_GO<sub>6.20</sub> membrane was 32, 40 and 18% higher than that for the pristine PES HF while using SiO<sub>2</sub> particles, BSA and sodium alginate as foulants, respectively.

#### 3.3 UV-treatment on SLGO to improve the antifouling performance of the membranes

In an attempt to further improve the antifouling performance, we conducted UV treatment on the SLGO flakes

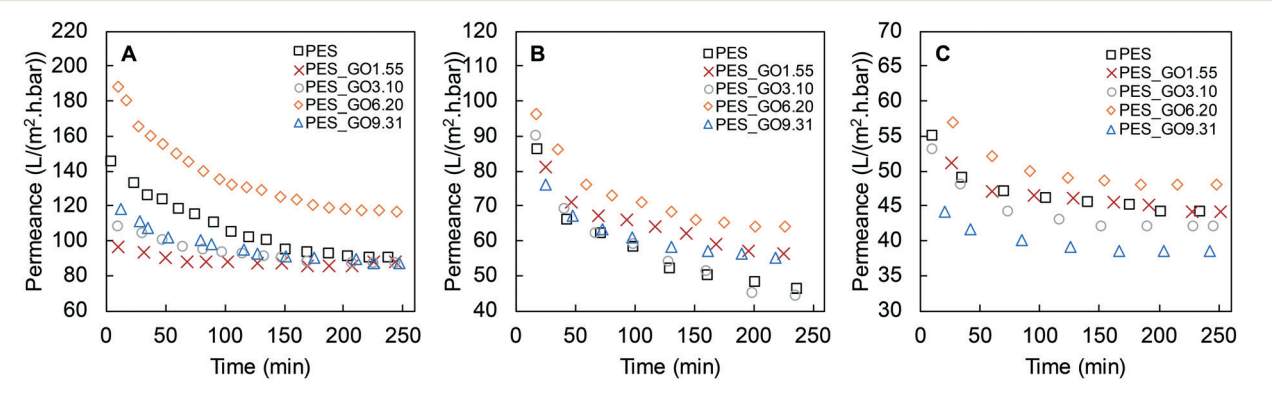


Fig. 6 The antifouling performance of SLGO coated PES hollow membranes using A) SiO<sub>2</sub> particles, B) BSA, and C) sodium alginate as model foulants.

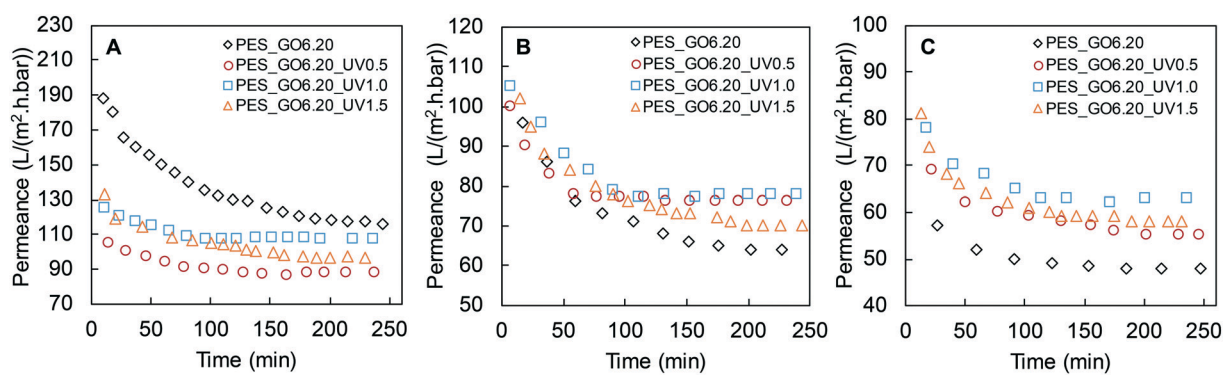


Fig. 7 The antifouling performance of PES hollow membranes while using A) SiO<sub>2</sub> particles, B) BSA, and C) sodium alginate as model foulants. Membranes were coated with SLGO flakes irradiated by UV light for different durations.

before coating on the PES HFs. According to the previous study of our group, UV-irradiation could introduce extra hydrophilic functional groups, such as carboxyl or hydroxyl groups, onto GO flakes. 18,22,29 Therefore, by depositing UVtreated SLGO on PES HFs, the additional hydrophilic functional groups on GO flakes could increase the overall hydrophilicity of the as-prepared PES HF membranes, and thus further improve the antifouling ability. Herein, we prepared PES HF membranes coated with SLGO flakes treated by UV light for different durations (0.5 to 1.5 h), and the UV-treated SLGO loading was fixed to 6.20 mg m<sup>-2</sup>. The effect of UVtreatment duration on the antifouling performance of the asprepared membranes was studied by fouling tests with the presence of the above three model foulants. As shown in Fig. 7, the antifouling ability of the PES HF membranes was significantly improved while being coated with UV-irradiated SLGO flakes.

When using SiO<sub>2</sub> particles as the model foulant, the permeance of the PES\_GO<sub>6.20</sub> membrane decreased around 30% during the filtration test. In contrast, the membranes deposited with UV-treated SLGO had lower initial permeance, which might be due to the accumulation of SiO2 on the membrane surface, but the permeance decreased to less than 15% (PES\_GO<sub>6.20</sub>\_UV<sub>1.0</sub>) for the whole testing process. Similar improvements were also observed when using BSA and sodium alginate as foulants. Moreover, when running the fouling test with BSA and sodium alginate, the PES HF membranes coated with UV-treated SLGO exhibited higher permeance, as shown in Fig. 7C; the permeance significantly increased from 54 L (m<sup>2</sup> h bar)<sup>-1</sup> to 65 L (m<sup>2</sup> h bar)<sup>-1</sup> when the membrane was coated with 1 h UV-treated SLGO flakes (PES\_GO<sub>6.20</sub>\_UV<sub>1.0</sub>). Overall, by comparing the antifouling ability of all the UVtreated membranes, membrane PES\_GO<sub>6.20</sub> UV<sub>1.0</sub> deposited with 6.20 mg m<sup>-2</sup> of 1 h UV-treated SLGO exhibited the best performance among other samples.

The PES\_GO<sub>6,20</sub> UV<sub>1,0</sub> HF membrane and the pristine PES HF were selected for the long-term antifouling test in MBR while using activated sludge supplied by the City's Metropolitan Wastewater Treatment Plant (Columbia, SC, USA). Fig. 8A shows that the permeate total organic carbon (TOC) concentration of the pristine PES HF and PES\_GO<sub>6.20</sub> UV<sub>1.0</sub> HF membranes was between 12 and 23 ppm, which means that the rejection for oxidized carbon is more than 99%, demonstrating good separation performance of both the PES HF and PES\_GO<sub>6,20</sub> UV<sub>1,0</sub> HF membranes. However, the transmembrane pressure of the pristine PES HF increased faster at a fixed permeate flux of 20 L m<sup>-2</sup> h<sup>-1</sup>. As illustrated in Fig. 8B, the transmembrane pressure of the PES HF drastically increased from 0.2 to 0.3 bar in the first 2 h, and then the pressure increase, from 0.3 to around 0.7 bar, gradually slows down in the next 50 h. In contrast, in the very first stage, it took about 6 h to increase the transmembrane pressure of

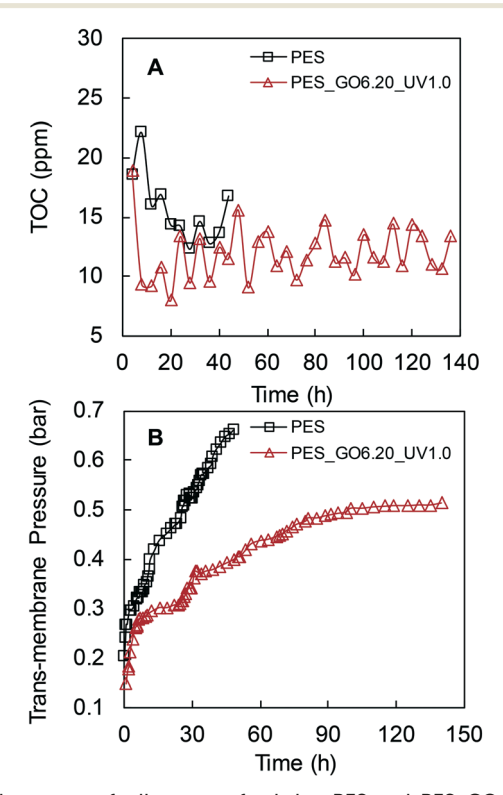
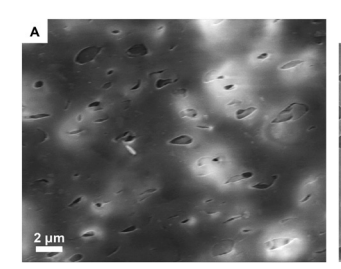


Fig. 8 Long term fouling test of pristine PES and PES\_ $GO_{6.20}$  UV<sub>1.0</sub> hollow fiber membranes in the MBR: (A) change of total organic carbon concentration in the permeate of the MBR with operation time; (B) the change of transmembrane pressure with operation time.



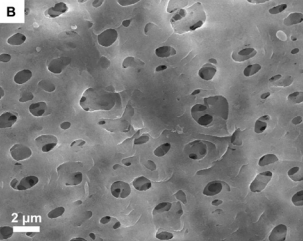


Fig. 9 The FESEM image of the fouled membrane after using in the MBR: (A) pristine PES HF after 2 days of use in the MBR; (B)  $PES\_GO_{6.20}\_UV_{1.0}$  HF membrane after 6 days of use in the MBR.

the PES\_GO<sub>6.20\_</sub>UV<sub>1.0</sub> membrane from 0.15 to 0.28 bar, and then the pressure slowly increased to 0.5 bar in 140 h, suggesting the greatly improved antifouling performance of this membrane.

Membrane surface morphology change after the test in the MBR was also examined by FESEM. As shown in Fig. 9A, the foulant layer has blocked most of the surface pores of the pristine PES HF, leaving only a negligible number of open pores for permeation. In contrast, the PES\_GO<sub>6.20</sub>\_UV<sub>1.0</sub> membrane surface had a negligible amount of foulant, and most of the surface pores were still open for permeation (Fig. 9B). This result is consistent with the excellent filtration performance of PES\_GO<sub>6.20</sub>\_UV<sub>1.0</sub> in MBR operation. The long-term MBR performance and FESEM images again confirmed that this UV-treated SLGO PES HF membrane could efficiently mitigate membrane fouling.

## 4. Conclusion

In this work, ultrathin SLGO deposited PES HF membranes were fabricated via a vacuum filtration method and used for MBR application. By using this facile vacuum filtration method, the PES HF surface can be selectively modified. Compared with other methods, 27,28 the membrane permeance and antifouling performance were significantly improved with only a small amount of SLGO loading, and the optimal SLGO loading was determined to be 6.20 mg m<sup>-2</sup>. To further increase membrane hydrophilicity, UV-treated SLGO flakes were deposited on PES HFs; the PES\_GO<sub>6.20</sub> UV<sub>1.0</sub> membrane, coated with 6.20 mg m<sup>-2</sup> of one hour UV-treated SLGO, exhibited excellent performance with a high water permeance of 65 L (m<sup>2</sup> h bar)<sup>-1</sup> and the lowest fouling (<15% permeance reduction). The long time MBR filtration test was conducted to compare the stable separation performance of the PES HF and PES\_GO<sub>6.20</sub> UV<sub>1.0</sub> membranes for real wastewater treatment. The transmembrane pressure for the pristine PES HF significantly increased to 0.7 bar after 50 h of testing. For the PES\_GO<sub>6.20</sub> UV<sub>1.0</sub> membrane, the transmembrane pressure slowly increased to around 0.5 bar and then a stable pressure was maintained for 150 h with similar rejection, suggesting that the UV-treated SLGO coating can not only lead to improved membrane filtration performance, but also increase energy efficiency and reduce operation cost.

# Conflicts of interest

The authors declare no competing financial interest.

# Acknowledgements

We gratefully acknowledge the support from the National Science Foundation (NSF) Career Award under Grant No. 1451887.

## References

- 1 G. T. Daigger, B. E. Rittmann, S. Adham and G. Andreottola, Are membrane bioreactors ready for widespread application?, *Environ. Sci. Technol.*, 2005, 39, 399a–406a.
- 2 X. Huang, C. H. Wei and K. C. Yu, Mechanism of membrane fouling control by suspended carriers in a submerged membrane bioreactor, J. Membr. Sci., 2008, 309, 7-16.
- 3 I. S. Kim and N. Jang, The effect of calcium on the membrane biofouling in the membrane bioreactor (MBR), *Water Res.*, 2006, 40, 2756–2764.
- 4 I. Sadeghi, P. Kaner and A. Asatekin, Controlling and Expanding the Selectivity of Filtration Membranes, *Chem. Mater.*, 2018, 30(21), 7328–7354.
- 5 I. Sadeghi, A. Aroujalian, A. Raisi, M. Fathizadeh and B. Dabir, Effect of solvent, hydrophilic additives and corona treatment on performance of polyethersulfone UF membranes for oil/water separation, *Procedia Eng.*, 2012, 44, 1539–1541.
- 6 Y. N. Yang, H. X. Zhang, P. Wang, Q. Z. Zheng and J. Li, The influence of nano-sized TiO2 fillers on the morphologies and properties of PSFUF membrane, *J. Membr. Sci.*, 2007, 288, 231–238.
- 7 S. Zinadini, A. A. Zinatizadeh, M. Rahimi, V. Vatanpour and H. Zangeneh, Preparation of a novel antifouling mixed matrix PES membrane by embedding graphene oxide nanoplates, J. Membr. Sci., 2014, 453, 292–301.
- 8 E. Celik, H. Park, H. Choi and H. Choi, Carbon nanotube blended polyethersulfone membranes for fouling control in water treatment, *Water Res.*, 2011, 45, 274–282.
- 9 J. H. Choi, J. Jegal and W. N. Kim, Fabrication and characterization of multi-walled carbon nanotubes/polymer blend membranes, *J. Membr. Sci.*, 2006, 284, 406–415.
- 10 K. Masoudnia, A. Raisi, A. Aroujalian and M. Fathizadeh, A hybrid microfiltration/ultrafiltration membrane process for treatment of oily wastewater, *Desalin. Water Treat.*, 2015, 55, 901–912.
- 11 V. Vatanpour, S. S. Madaeni, A. R. Khataee, E. Salehi, S. Zinadini and H. A. Monfared, TiO2 embedded mixed matrix PES nanocomposite membranes: Influence of different sizes and types of nanoparticles on antifouling and performance, *Desalination*, 2012, 292, 19–29.
- 12 M. H. Gu, J. E. Kilduff and G. Belfort, High throughput atmospheric pressure plasma-induced graft polymerization for identifying protein-resistant surfaces, *Biomaterials*, 2012, 33, 1261–1270.

- 13 J. Huang, K. S. Zhang, K. Wang, Z. L. Xie, B. Ladewig and H. T. Wang, Fabrication of polyethersulfone-mesoporous silica nanocomposite ultrafiltration membranes with antifouling properties, J. Membr. Sci., 2012, 423, 362-370.
- 14 R. Z. Pang, X. Li, J. S. Li, Z. Y. Lu, X. Y. Sun and L. J. Wang, Preparation and characterization of ZrO2/PES hybrid ultrafiltration membrane with uniform ZrO2 nanoparticles, Desalination, 2014, 332, 60-66.
- 15 I. Sadeghi, A. Aroujalian, A. Raisi, B. Dabir and M. Fathizadeh, Surface modification of polyethersulfone ultrafiltration membranes by corona air plasma for separation of oil/water emulsions, J. Membr. Sci., 2013, 430, 24-36.
- 16 I. Sadeghi, J. Kronenberg and A. Asatekin, Selective Transport through Membranes with Charged Nanochannels Formed by Scalable Self-Assembly of Random Copolymer Micelles, ACS Nano, 2018, 12, 95-108.
- 17 I. Sadeghi, H. Yi and A. Asatekin, A Method for Manufacturing Membranes with Ultrathin Hydrogel Selective Layers for Protein Purification: Interfacially Initiated Free Radical Polymerization (IIFRP), Chem. Mater., 2018, 30, 1265-1276.
- 18 Y. Huang, H. Li, L. Wang, Y. L. Qiao, C. B. Tang, C. I. Jung, Y. M. Yoon, S. G. Li and M. Yu, Ultrafiltration Membranes with Structure-Optimized Graphene-Oxide Coatings for Antifouling Oil/Water Separation, Adv. Mater. Interfaces, 2015, 2, 1400433.
- 19 K. Masoudnia, A. Raisi, A. Aroujalian and M. Fathizadeh, Treatment of Oily Wastewaters Using the Microfiltration Process: Effect of Operating Parameters and Membrane Fouling Study, Sep. Sci. Technol., 2013, 48, 1544-1555.
- 20 M. Fathizadeh, H. N. Tien, K. Khivantsev, J. T. Chen and M. Yu, Printing ultrathin graphene oxide nanofiltration membranes for water purification, J. Mater. Chem. A, 2017, 5, 20860-20866.
- 21 M. Fathizadeh, W. W. L. Xu, F. L. Zhou, Y. Yoon and M. Yu, Graphene Oxide: A Novel 2-Dimensional Material in Membrane Separation for Water Purification, Adv. Mater. Interfaces, 2017, 4, 1600918-1600934.
- 22 F. L. Zhou, M. Fathizadeh and M. Yu, Single- to Few-Layered, Graphene-Based Separation Membranes, Annu. Rev. Chem. Biomol. Eng., 2018, 9, 17-39.
- 23 F. L. Zhou, H. N. Tien, W. W. L. Xu, J. T. Chen, Q. L. Liu, E. Hicks, M. Fathizadeh, S. G. Li and M. Yu, Ultrathin graphene oxide-based hollow fiber membranes with brushlike CO2-philic agent for highly efficient CO2 capture, Nat. Commun., 2017, 8, 2107.
- 24 W. L. W. Xu, F. L. Zhou and M. Yu, Tuning Water Nanofiltration Performance of Few-Layered, Reduced

- Graphene Oxide Membranes by Oxygen Plasma, Ind. Eng. Chem. Res., 2018, 57, 16103-16109.
- 25 W. W. L. Xu, C. Fang, F. L. Zhou, Z. N. Song, Q. L. Liu, R. Qiao and M. Yu, Self-Assembly: A Facile Way of Forming Ultrathin, High-Performance Graphene Oxide Membranes for Water Purification, Nano Lett., 2017, 17, 2928-2933.
- 26 Y. Z. Qin, Y. Y. Hu, S. Koehler, L. H. Cai, J. J. Wen, X. J. Tan, W. W. L. Xu, Q. Sheng, X. Hou, J. M. Xue, M. Yu and D. Weitz, Ultrafast Nanofiltration through Large-Area Single-Layered Graphene Membranes, ACS Appl. Mater. Interfaces, 2017, 9, 9239-9244.
- 27 J. Lee, H. R. Chae, Y. J. Won, K. Lee, C. H. Lee, H. H. Lee, I. C. Kim and J. M. Lee, Graphene oxide nanoplatelets composite membrane with hydrophilic and antifouling properties for wastewater treatment, J. Membr. Sci., 2013, 448, 223-230.
- 28 F. M. Jin, W. Lv, C. Zhang, Z. J. Li, R. X. Su, W. Qi, Q. H. Yang and Z. M. He, High-performance ultrafiltration membranes based on polyethersulfone-graphene oxide composites, RSC Adv., 2013, 3, 21394-21397.
- 29 H. Li, Y. Huang, Y. T. Mao, W. W. L. Xu, H. J. Ploehn and M. Yu, Tuning the underwater oleophobicity of graphene oxide coatings via UV irradiation, Chem. Commun., 2014, 50, 9849-9851.
- 30 B. K. Hwang, W. N. Lee, K. M. Yeon, P. K. Park, C. H. Lee, I. S. Chang, A. Drews and M. Kraume, Correlating TMP increases with microbial characteristics in the bio-cake on the membrane surface in a membrane bioreactor, Environ. Sci. Technol., 2008, 42, 3963-3968.
- 31 I. Sadeghi, P. Arbab, M. Fathizadeh, H. Fakhraee and M. Amrollahi, Optimization of Nano-TiO2 Photocatalytic Reactor for Organophosphorus Degradation, Adv. Mater. Sci. Eng., 2012, 2012, 510123.
- 32 K. H. Chu, M. Fathizadeh, M. Yu, J. R. V. Flora, A. Jang, M. Jang, C. M. Park, S. S. Yoo, N. Her and Y. Yoon, Evaluation of Removal Mechanisms in a Graphene Oxide-Coated Ceramic Ultrafiltration Membrane for Retention of Natural Organic Matter, Pharmaceuticals, and Inorganic Salts, ACS Appl. Mater. Interfaces, 2017, 9, 40369-40377.
- 33 M. Fathizadeh, H. N. Tein, K. Khivantsev, Z. Song, F. Zhou and M. YU, Polyamide/nitrogen-doped graphene oxide quantum dots (N-GOQD) thin film nanocomposite reverse osmosis membranes for high flux desalination, Desalination, 2019, 451, 125-132.
- 34 F. Zhou, H. N. Tien, Q. Dong, W. L. Xu, H. Li, S. Li and M. Yu, Ultrathin, ethylenediamine-functionalized graphene oxide membranes on hollow fibers for CO2 capture, J. Membr. Sci., 2019, 573, 184-191.